Heterogeneous & Homogeneous & Bio- & Nano-

CHEMCATCHEM

CATALYSIS

Accepted Article

Title: Facile synthesis of high performance NiPd@CMK-3 nanocatalyst for mild Suzuki-Miyaura coupling reactions

Authors: Ji Chan Park, Aram Kim, Sanha Jang, Jung-Il Yang, Shin Wook Kang, Chan-Woo Lee, Byung-Hyun Kim, and Kang Hyun Park

To be cited as: *ChemCatChem* 10.1002/cctc.201801872

Link to VoR: http://dx.doi.org/10.1002/cctc.201801872

A Journal of

ChemPubSoc Europe

WILEY-VCH

www.chemcatchem.org

10.1002/cctc.201801872

WILEY-VCH

COMMUNICATION

Facile synthesis of high performance NiPd@CMK-3 nanocatalyst for mild Suzuki-Miyaura coupling reactions

Ji Chan Park,[‡a] Aram Kim,[‡b] Sanha Jang,[b] Jung-Il Yang,[a] Shin Wook Kang,[a] Chan-Woo Lee,[c] Byung-Hyun Kim,[*,c] Kang Hyun Park[b,*]

Abstract: Highly dispersed nickel-palladium bimetallic nanoparticles (~2 nm) on ordered mesoporous carbon CMK-3 (NiPd@CMK-3) were simply prepared using a co-infiltration method of the metal salts. The nanoparticles were successfully applied to the mild Suzuki-Miyaura coupling reactions at 25 ~ 50 °C using 4-bromoanisole and phenylboronic acid, and showed excellent catalytic performance with the high activity (0.521×10^{-3} $mol_c \cdot g_{am}^{-1} \cdot s^{-1}$) and productivity (69.1 $g_p \cdot g_{cat}^{-1} \cdot h^{-1}$).

Due to their easy separation, good reusability, and environmental compatibility, solid catalysts have been widely used in various organic reactions.[1] Many studies on catalyst synthesis have been performed to enhance the catalyst activity and stability by manipulating morphology and active sites, but maximization of catalyst productivity still remains as a challenge in the heterogeneous catalytic reactions.[2-5] To find a high performance catalyst, high dispersion of active nanoparticles and high load of active metals are necessary, and can generally be achieved by well-defined physical protection materials such as metal-oxides (silica, alumina, and titania) and carbons (carbon nanotube, graphene, and activated carbon) to prevent active particle aggregation and agglomeration.[6-10]

The Suzuki-Miyaura coupling reaction, which creates new carbon-carbon bonds between organohalides and boronic acid derivatives, has been utilized for the production of fine chemicals, polymers, and pharmaceutical products, using palladium (Pd)-based catalysts in alkaline condition.[11-13] Typically, heterogeneous Pd nanocatalysts such as Pd nanoparticles (NPs), Pd/C, Pd/SiO_2, and Pd/Al_2O_3 have been applied to the reaction.[14-19] Recently, an ordered mesoporous carbon (CMK-3) with high surface areas, pore volumes, and uniform pore sizes has been introduced as a catalyst support, providing good reactant diffusion surroundings and enhanced durability for the active sites.[20,21]

In heterogeneous catalytic reactions, increase of product yield per unit the catalyst weight has a significant meaning from a practical aspect. Therefore, highly metal-loaded catalysts (above 20 wt%) are needed with high and uniform dispersion on a support; such materials have large pore volume and porosity, leading to an increased number of active sites. However, noble metals are generally restricted to low load of the active sites, mainly due to their high prices. Reducing dosage of expensive Pd metal has been a major challenge for an economical reasons.[22-25] In particular, mixing other elements with the precious Pd metal can modulate the elemental distribution on the surface, the intermetallic charge transfer, and the lattice strain.[26-28] In recent years, NiPd bimetallic particles have shown their enhanced catalytic activity, even higher than that of single metal Pd particles, for carbon coupling reactions.[29-33] Although the results for synergistic effects of NiPd nanoparticles in carbon coupling reactions have been reported, the mechanisms and theoretical explanations for the enhanced activity of NiPd alloys are rare and still ambagious.[34,35] In addition, the preparation processes for NiPd bimetallic nanostructures are complicated.[36,37]

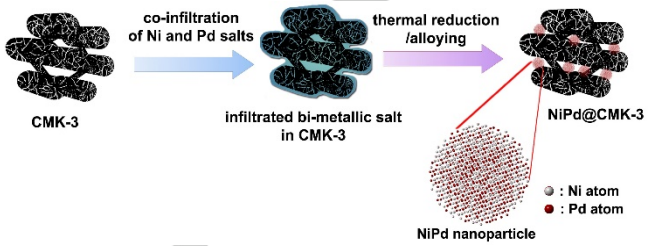

Scheme 1. Synthetic procedures for NiPd@CMK-3 nanocatalyst.

Herein, we report a new synthetic method for surfactant-free NiPd bimetallic nanoparticles with high dispersion and high content of active sites (20 wt%) in the pores of CMK-3. The catalyst shows good activity of 0.521×10^{-3} $mol_c \cdot g_{am}^{-1} \cdot s^{-1}$ under the mild Suzuki-Miyaura coupling reaction at 25 °C, as well as very high productivity (69.1 $g_p \cdot g_{cat}^{-1} \cdot h^{-1}$) compared to those of other conventional catalysts. Furthermore, the high catalytic property of the NiPd bimetallic surfaces can be interpreted based on computational simulations.

First, CMK-3 was prepared using a silica template SBA-15, as reported in elsewhere.[38] Next, the NiPd bimetallic nanoparticles were easily synthesized via a simultaneous infiltration of nickel nitrate hexahydrate and palladium nitrate dihydrate into the pores of the CMK-3 and subsequent thermal reduction under a hydrogen gas flow (Scheme 1). During the process, it was possible to form the nanoparticles through the pore confinement effect. The TEM image shows extremely tiny NiPd nanoparticles as black dots in the nano-channels of CMK-3 (Figure 1a). The high-resolution TEM (HRTEM) image indicates the uniform NiPd nanoparticles around 2 nm (Figure 1b). The distance between adjacent lattice fringe images was measured and found to be 0.22 nm, which corresponded to the (111) plane of face-centered-cubic (fcc) NiPd alloy (Figure 1c). The high-angle annular dark-field

[a] Dr. J. C. Park, Dr. J.-I. Yang, Dr. S. W. Kang,
Clean Fuel Laboratory,
Korea Institute of Energy Research, Daejeon, 34129, Korea
[b] Dr. A. Kim, S. Jang, Prof. K. H. Park
Department of Chemistry and Chemistry Institute for Functional Materials,
Pusan National University, Busan, 46241, Korea
E-mail: chemistry@pusan.ac.kr
[c] Dr. C. W. Lee, Dr. B. H. Kim,
Platform Technology Laboratory,
Korea Institute of Energy Research, Daejeon, 34129, Korea
E-mail: bhkim@kier.re.kr
‡ These authors contributed equally to this work.
Supporting information for this article is given via a link at the end of the document.

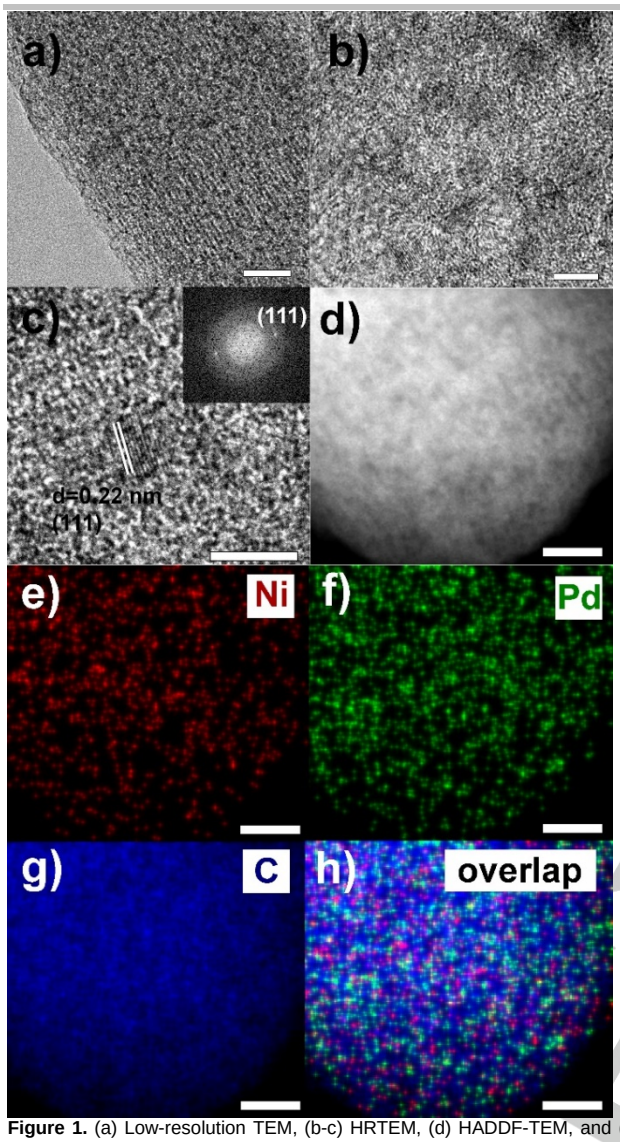

Figure 1. (a) Low-resolution TEM, (b-c) HRTEM, (d) HADDF-TEM, and (e-h) scanning TEM images with elemental mapping (Ni, Pd, C, and all) of NiPd@CMK-3 nanocatalyst. The bars represent 50 nm (a, d-h) and 5 nm (b, c).

(HAADF)-TEM and the corresponding elemental mapping images of NiPd@CMK-3 nanocatalyst demonstrate high dispersity of Ni and Pd elements incorporated throughout the mesopores of CMK-3 (Figure 1d-h). After thermal treatment, Pd and Ni were each loaded at 10 wt% on the basis of the metals converted from the metal salts.

For comparison of the characteristics of NiPd@CMK-3, the Ni@CMK-3 and Pd@CMK-3 nanocatalysts were also prepared by sole infiltration of the single metal salt with each metal having a loading amount of 10 wt%. The TEM and HAADF-TEM images show the Ni nanoparticles with diameters of approximately 2 nm; nanoparticles are well-incorporated in the pores of CMK-3 (Figure 2a-b). The Pd nanoparticles, incorporated into the mesopores of CMK-3, were observed to be around 3 nm (Figure 2c-d). The phases and crystallite sizes of Ni@CMK-3, Pd@CMK-3, and NiPd@CMK-3 nanocatalysts were analysed using X-ray diffraction (XRD) spectra (Figure 2e). The XRD patterns of the Ni@CMK-3 and Pd@CMK-3 were indexed to the face-centered-cubic (fcc) Ni (JCPDS No. 04-0850) and fcc Pd (JCPDS No. 46-1043), respectively. The diffraction peak of NiPd@CMK-3 was

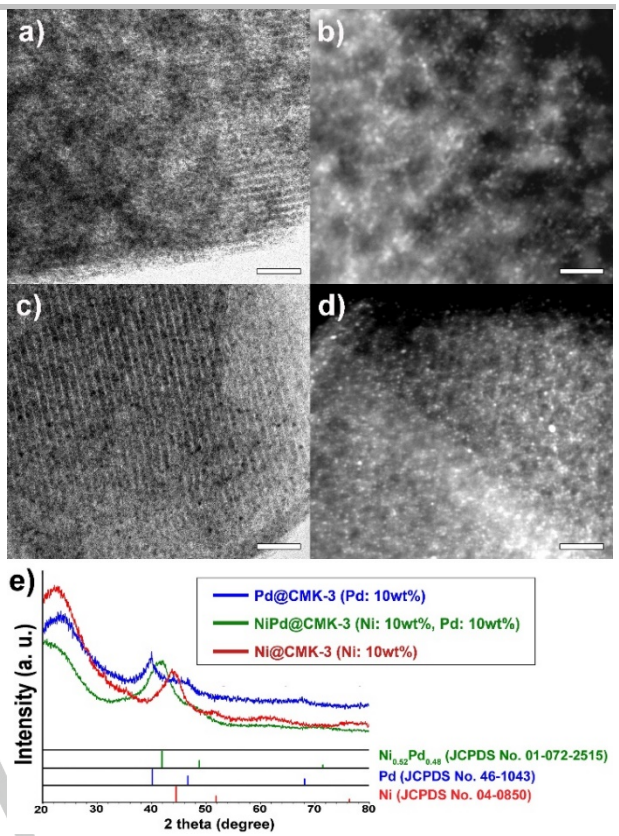

Figure 2. (a) TEM and (b) HAADF-TEM images of Ni@CMK-3, (c) TEM and (d) HAADF-TEM images of Pd@CMK-3, and (e) XRD spectra of Ni@CMK-3, Pd@CMK-3, and NiPd@CMK-3 catalysts. All bars represent 50 nm.

observed between $2\theta = 40.1^{o}$ of Pd (111) and 44.5^{o} of Ni (111). This shift indicates Pd lattice contraction caused by replacing fcc Pd atoms with Ni atoms. Using the Scherrer equation, the crystal sizes of Ni, Pd, and NiPd nanoparticles in the catalysts were calculated and found to be 1.5, 2.8, 1.6 nm, respectively. These values are well-matched to the particle sizes in the TEM images.

To characterize the porous structures of the catalyst, the N_2 adsorption/desorption isotherms were obtained. Both the pristine CMK-3 and NiPd@CMK-3 exhibited type IV adsorption–desorption hysteresis, indicating preservation of the mesoporous structure after NiPd formation in CMK-3 (Figure 3a). The BET surface areas and total pore volumes were 1433.5 $m^2 \cdot g^{-1}$ and 1.45 $cm^3 \cdot g^{-1}$ for the CMK-3, and 862.4 $m^2 \cdot g^{-1}$ and 0.91 $cm^3 \cdot g^{-1}$ for the NiPd@CMK-3 nanocatalyst. Using the Barrett–Joyner-Halenda (BJH) method, average pore sizes of CMK-3 and NiPd@CMK-3 were estimated from the desorption branches of N_2 isotherms and found to be equal at 5.3 nm (Figure 3b). The alloyed NiPd loading of the NiPd@CMK-3 was 18.74 wt% (Ni: 9.71 wt%, Pd: 9.03 wt%), as determined by inductively coupled plasma-atomic emission spectrometry (ICP-AES), which is a good match with the nominal metal loading value of 20 wt%.

The CMK-3 supported NiPd bimetallic nanoparticles were employed in the Suzuki-Miyaura coupling reactions. First, the reactions using 4-bromoanisole and phenylboronic acid were performed with screening some solvents and bases under different temperature conditions (Table S1-2, see the ESI†). Methanol and ethanol as protic solvents led to higher conversions of 4-bromoanisole as a substrate than those of other organic solvents such as dimethylformamide (DMF), dimethyl sulfoxide (DMSO), dimethylacetamide (DMAc), 1,4-dioxane, acetonitrile,

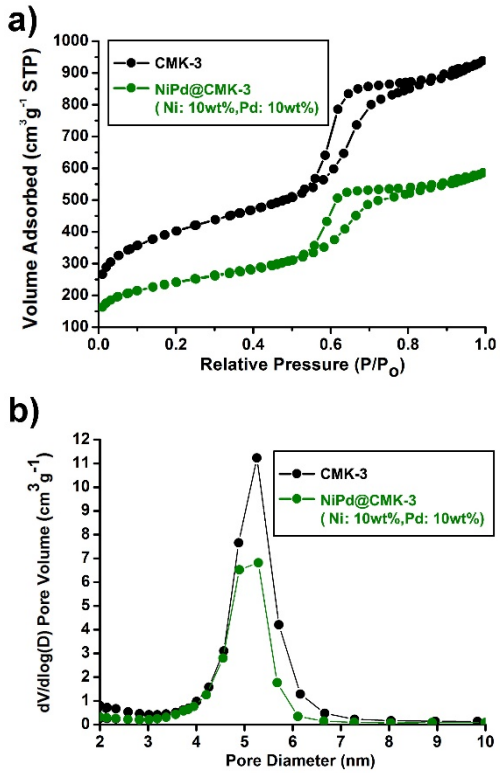

Figure 3. (a) N_2 adsorption/desorption isotherms of pristine CMK-3 and NiPd@CMK-3, and (b) pore size distribution diagrams calculated from desorption branches using the BJH method.

toluene, and tetrahydrofuran. Using mixed solvents with water, conversion rates were found to increase more, because water as a co-solvent can facilitate dissolution of K_2CO_3 as a base and contribute to protolytic decomposition of an organoboron compounds. In the base effect, KOH and NaOH, which are highly soluble in water, showed high conversion rates (> 96%), compared to the value (72 %) of $KHCO_3$ and $NaHCO_3$. As expected, higher conversion rates were obtained, increasing the reaction temperatures in the range of 25–75 °C.

Furthermore, several substrates for the Suzuki-Miyaura coupling reactions were tested using several aryl halides and aryl boronic acid. The NiPd@CMK-3 nanocatalyst exhibited high conversion rates (>92%) for various aryl halides and aryl boronic acid substitutes involving electron-withdrawing and electron-donating groups (Table 1). Bromobenzenes bearing methyl, hydroxyl, fluoride, and aldehyde, and phenylboronic acid with substituents were successfully converted to the biaryl products.

To compare the activity of NiPd@CMK-3 nanocatalyst, Pd (20 wt%)@CMK-3 was tested under the same reaction conditions (Figure 4a). The catalyst activity was noted to exhibit site-time-yield (the number of 4-bromoanisole moles converted to 4-methoxybiphenyl per gram of active metals per second). For the NiPd@CMK-3 catalyst containing 20 wt% of NiPd alloy, the activity was calculated to be 0.521 $mmol \cdot g_{am}^{-1} \cdot s^{-1}$ higher than the activity (0.495 $mmol \cdot g_{am}^{-1} \cdot s^{-1}$) of pure Pd@CMK-3 (Pd: 20wt%) (Figure 4b). To the best of our knowledge, this is a record-high value among the reported activity data so far (Table S3). The catalyst productivity [product yield (g) per catalyst weight (g) per hour] was calculated. As expected, the NiPd@CMK-3 catalyst showed a high productivity (69.1 $g_p \cdot g_{cat}^{-1} \cdot h^{-1}$) (Figure 4c). The catalyst had a much higher value than those of other previously

Table 1. Suzuki-Miyaura reaction data using the NiPd@CMK-3 nanocatalyst for various aryl halides and aryl boronic acids.[a)]

Entry	Aryl halide	Aryl boronic acid	Conversion (%)
1	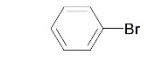	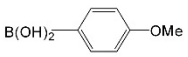	>99.9
2	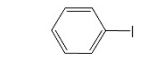	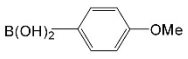	97
3	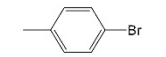	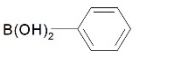	>99.9
4	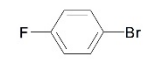	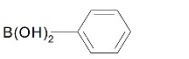	>99.9
5	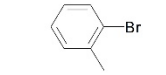	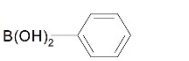	95
6	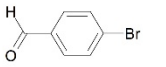	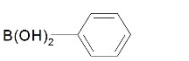	>99.9
7	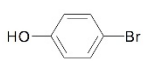	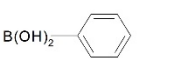	>99.9
8	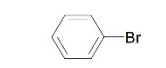	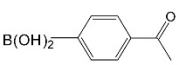	98
9	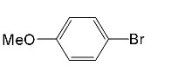	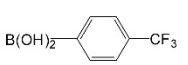	92
10	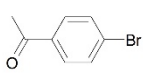	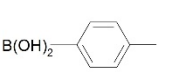	>99.9
11	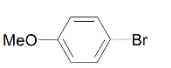	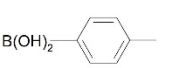	96

a) The reaction tests were conducted at 50 °C for 1h with aryl halide (0.5 mmol), arylboronic acid (0.6 mmol), K_2CO_3 (1.0 mmol), NiPd@CMK-3 (2.7 mg), and ethanol/H_2O (1:1). Conversion rates were determined using GC-MS spectrometry.

previously reported other catalysts (0.2 ~ 28.2 $g_p \cdot g_{cat}^{-1} \cdot h^{-1}$, Table S3). On the other hand, the Pd based catalysts showed the lower productivity values [56.3 $g_p \cdot g_{cat}^{-1} \cdot h^{-1}$ at Pd(10 wt%)@CMK-3, 65.7 $g_p \cdot g_{cat}^{-1} \cdot h^{-1}$ at Pd(20 wt%)@CMK-3, Table S3].

Although the active metal contents (Ni: 10wt%, Pd: 10wt%) in the NiPd@CMK-3 nanocatalyst were high compared to those of the conventional catalysts, the high activity of the catalyst due to the small and active NiPd bimetallic nanoparticles in CMK-3 can lead to the enhanced productivity, making this material very advantageous for future commercial applications.

To understand the origin of higher activity of the NiPd@CMK-3 nanocatalyst in the Suzuki-Miyaura coupling reaction, the catalytic property of the NiPd@CMK-3 nanocatalyst was newly elucidated by theoretical data based on computational simulations. Electronic structure and charge transfer calculations were performed using the density functional theory (DFT). Generally, it is known that the synergetic effects in bimetallic alloys can be ascribed to the modified electronic structures and the corresponding charge transfer mechanism.

Model structures for Pd nanocatalyst as a reference model and two representative bimetallic NiPd nanocatalysts were prepared: 1) a clean Pd (111) surface, 2) a Pd (111) surface where a Ni layer

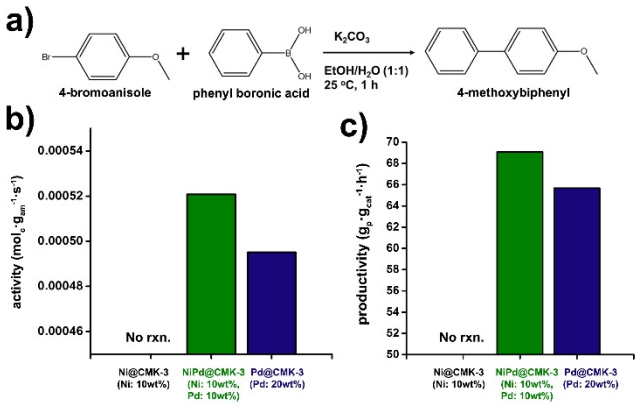

Figure 4. (a) Applied Suzuki-Miyaura coupling reaction, and (b) catalytic activity and (c) productivity data of the catalysts. The reactions were conducted with 4-bromoanisole (1.25 mmol), phenylboronic acid (1.50 mmol) and K_2CO_3 (2.50 mmol) at 25 °C for 1 h. (g_{am}= active metal content, mol_c=converted 4-bromoanisole mol, g_p=product weight, g_{cat}=total weight of active metal and supporting material)

is located below a surface layer of Pd, and 3) a Pd (111) surface covered with a Ni layer (Figure S1). Then, a 4-bromoanisole molecule was placed on the surfaces of our model structures since the first step of the Suzuki-Miyaura coupling reaction should be an adsorption of 4-bromoanisole on the surfaces of catalysts [34]. It is also known that the first step which is the oxidative addition of an aryl halide to a catalyst is generally the rate determining step of the reaction.[39] The adsorption site was chosen to be the hollow-hcp site, which is the most stable adsorption site among the hollow-fcc, hollow-hcp, bridge and parallel sites (Table S4). The adsorption site was chosen to be the hollow-fcc site. The adsorption energy of 4-bromoanisole on different surfaces, E_{ads}, was calculated using the following equation:

$$E_{ads} = E_{(bromoanisole/substrate)} - [E_{(bromoanisole)} + E_{(substrate)}]$$

where $E_{(bromoanisole/substrate)}$ is the total energy of the system after an adsorption of 4-bromoanisole, $E_{(bromoanisole)}$ is the energy of an isolated 4-bromoanisole molecule, and $E_{(substrate)}$ is the energy of a clean surface. The calculated E_{ads} of the bimetallic NiPd surfaces was –0.51 eV for Pd covered NiPd (111) and –0.80 eV for Ni covered NiPd (111), respectively, while E_{ads} for the clean Pd surface was –0.42 eV (Table 2). Since the chemical reaction start with the adsorption process, the higher E_{ads} could be beneficial to the reaction.[40]

The theoretical results of adsorption energy calculations are in good agreement with the experimental results showing the higher activity of the NiPd@CMK-3 nanocatalyst than that of the Pd nanocatalyst in the Suzuki-Miyaura coupling reaction. To clarify the observed adsorption behaviors, we further quantified the charge transfer from the substrate to Br in the 4-bromoanisole molecule. The charge differences of Br between before and after the adsorption of bromoanisole were found to be –0.002 e, –0.044 e, and –0.110 e for clean Pd (111), Pd covered NiPd (111), and Ni covered NiPd (111) and, respectively. Consequently, the more charges transferred from the substrate to Br in 4-bromoanisole, the stronger adsorption of 4-bromoanisole on the catalysts occurs, so that the bimetallic NiPd nanocatalysts are energetically more favorable for the first step of the Suzuki-Miyaura coupling reaction, leading to the higher activity (Figure 5).

Table 2. Adsorption energies of 4-bromoanisole on different surfaces and charge differences of Br before/after the adsorption.

System	E_{ads} (eV)	Δ Charge (e, Bader)	
		Br	Substrate
Pd (111)	–0.42	–0.002	+0.034
Pd covered NiPd (111)	–0.51	–0.044	+0.062
Ni covered NiPd (111)	–0.80	–0.110	+0.061

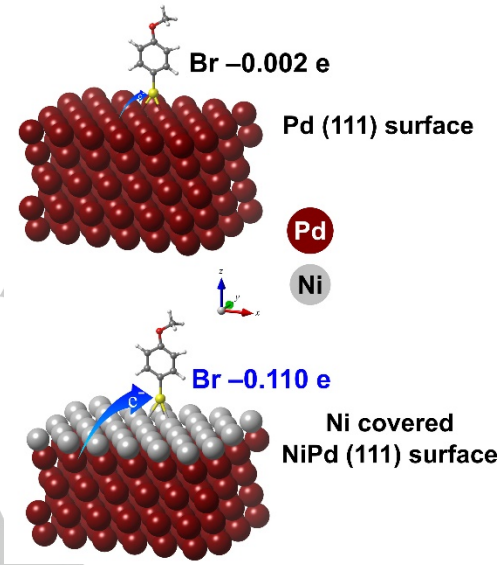

Figure 5. Geometry optimized structures for 4-bromoanisole adsorbed on a Pd (111) surface and a Ni covered NiPd (111) substrate. The blue arrow is a schematic diagram indicating a direction and an amount of electron charge transfer from the substrate to Br in 4-bromoanisole. The number next to the Br atom (yellow) is the Bader charge difference before and after the adsorption.

To check the catalyst stability and recyclability, the NiPd@CMK-3 nanocatalyst was separated after reaction. The NiPd/CMK-3 nanocatalysts were run four times. Although gradual and partial degradation was revealed, the rapid deactivation was not detected. The conversion rates were gradually decreased from >99% of the fresh catalyst to ~84% of the recovered catalyst applied in the 4th run (Figure S2). It would be attributed to the reduced active surface areas by increased particle sizes (Figure S2c). The partially dissolved NiPd alloy particles during the reaction led to the formation of more increased particles compared to the original particles as shown in Figure S2a-c.

Conclusions

In conclusion, the NiPd@CMK-3 nanocatalyst, bearing surfactant-free NiPd nanoparticles (2 nm), was simply prepared with a co-infiltration of mixed metal salts and subsequent thermal treatment. The high metal load (Ni: 10 wt%, Pd: 10 wt%) and dispersion of the catalyst could contribute to increased productivity and to securing the particle stability for the Suzuki-Miyaura coupling reactions. In addition, from the result of the computational simulations, it was revealed that the NiPd bimetallic particles had a stronger adsorption characteristic, with higher charge transfer to 4-bromoanisole, than that of solitary Pd particles, supporting the experimental data. It is anticipated that this synthetic strategy for bimetallic NiPd will be applied to other transition metal-noble metal hybrid nanocatalysts, such as CMK-3 supported CoPd, FePd, NiPt, etc., for catalytic reactions.

Experimental Section

Materials and methods

Chemicals Pluronic P123 (Mw=5,800), tetraethyl orthosilicate (TEOS, 98%), hydrofluoric acid (HF, 48 wt%), nickel nitrate hexahydrate ($Ni(NO_3)_2{\cdot}6H_2O$, ACS reagent, ≥98%), palladium(II) nitrate dihydrate ($Pd(NO_3)_2{\cdot}2H_2O$, ~ 40% Pd basis), sucrose and were purchased from Aldrich. Hydrochloric acid (HCl, 35 wt%) and sulfuric acid (H2SO4, 95 wt%) were purchased from Junsei. All chemicals were used as received without further purification..

Preparation of CMK-3 The mesoporous carbon (CMK-3) was prepared by replication of mesoporous silica template (SBA-15). The SBA-15 was prepared using a hydrothermal method. Typically, pluronic P123 (16.0 g) was dissolved in distilled water (120 g) and HCl (2.0 M, 480 g) solution with stirring at 35 °C for 1 h. TEOS (34.0 g) was added into the mixture solution and aged for 24 h at 40 °C. After that, the reaction mixture was then transferred to a Teflon-lined autoclave and aged at 150 °C for 24 h. White powder was recovered through filtration and subsequently washed with water, ethanol, and acetone. The product was completely dried in an oven at 100 °C for 6 h, and was calcined at 550°C for 5 h in air to yield SBA-15. The obtained SBA-15 (3.0 g) was added into the carbon precursor solution prepared by dissolving sucrose (4.1 g) and H_2SO_4 (0.5 g) in distilled water (15.0 g). The mixture was placed in an oven at 100°C for 6 h and subsequently aged at 160 °C for 2 h. After that, sucrose (2.5 g), H_2SO_4 (0.3 g), and distilled water (15.0 g) were additionally added into the aged mixture. The sample was carbonized at 800°C and maintained at that temperature for 2 h under N_2 flow (0.2 $L{\cdot}min^{-1}$). Finally, to remove the silica template, the carbon–silica composite was washed with HF solution (2.0 M, 100 g) at room temperature. The product was filtered, washed with ethanol, and thermally treated at 400 °C for 4 h under N_2 flow (0.2 $L{\cdot}min^{-1}$).

Synthesis of NiPd@CMK-3 nanocatalyst To prepare the Ni(10wt%)Pd(10wt%)@CMK catalyst, $Ni(NO_3)_2{\cdot}6H_2O$ (0.310 g) and $Pd(NO_3)_2{\cdot}2H_2O$ (0.156 g) were dissolved in distilled water (0.3 mL). The mixed solution was dropped on CMK-3 powder (0.5 g) and infiltrated by grinding the mixture in a mortar for several minutes under ambient conditions. Then, the mixed powders were placed into a 30 mL polypropylene bottle and aged at 60 °C in an oven. After aging for 24 h, the sample was cooled in an ambient atmosphere and transferred to an alumina boat in a tube-type furnace. Finally, under a H_2 flow of 0.2 $L{\cdot}min^{-1}$, the NiPd-incorporated CMK-3 powder was slowly heated to 350 °C at a ramping rate of 2.7 $°C{\cdot}min^{-1}$. The sample was thermally treated at 350 °C for 4 h under the continuous H_2 flow.

Synthesis of Pd@CMK-3 and Ni@CMK-3 To prepare the Pd(10wt%)/CMK-3 catalyst, aqueous Pd nitrate solution (1.74 M, 0.3 mL) was dropped on CMK-3 powder (0.5 g) and infiltrated by grinding the mixture in a mortar for several minutes under ambient condition until the powder was homogeneously black. Then, the mixed powders were placed in a polypropylene bottle and aged at 60 °C in an oven. After aging for 24 h, the sample was cooled in an ambient atmosphere and transferred to an alumina boat in a tube-type furnace. Finally, under a H_2 flow of 0.2 $L{\cdot}min^{-1}$, the Pd-incorporated CMK-3 powder was slowly heated to 350 °C at a ramping rate of 2.7 $°C{\cdot}min^{-1}$. The sample was thermally treated at 350 °C for 4 h under the continuous H_2 flow. For the preparation of the Ni(10wt%)@CMK-3 nanocatalyst, all procedures were identical to those used in the synthesis of Pd(10wt%)@CMK-3, except for the use of aqueous Ni nitrate solution (6.3 M, 0.3 mL) and CMK-3 (1.0 g). For the preparation of the Pd(20wt%)@CMK-3 nanocatalyst, all procedures were identical to those used in the synthesis of Pd(10wt%)@CMK-3, except for the use of aqueous Pd nitrate solution (3.92 M, 0.3 mL).

Suzuki coupling reaction tests For the typical reaction test, the catalyst, 4-bromoanisole, phenylboronic acid, ethanol, water, and potassium carbonate were added to a 10 mL glass vial with an aluminium seal. The mixture was vigorously stirred for 1 h. After that, the reaction mixture was filtered, washed with saturated aqueous sodium bicarbonate solution, and extracted with dichloromethane. The organic layer was concentrated under reduced pressure. The conversion rate of 4-bromoanisole was determined using gas chromatography-mass (GC-MS) spectrometry.

Characterization High resolution transmission electron microscopy (TEM) analysis was performed using a Tecnai TF30 ST and a Titan Double Cs corrected TEM (Titan cubed G2 60-300). Energy-dispersive X-ray spectroscopy (EDS) elemental mapping data were collected using a higher efficiency detection system (Super-X detector). High power powder-XRD (Rigaku D/MAX-2500, 18 kW) was also used for the analysis. N_2-sorption isotherms were obtained at 77 K with a Tristar II 3020 surface area analyser.

Acknowledgements

This research was supported by the Research and Development Program of the Korea Institute of Energy Research (KIER) (No. B9-2461-01) and funded by the Ministry of Trade, Industry and Energy (MOTIE) of the Republic of Korea (No. 10050509). A. Kim and K. H. Park were supported by Basic Science Research Program through the National Research Foundation of Korea (NRF) funded by the Ministry of Science, ICT & Future Planning (2017R1A4A1015533 and 2017R1D1A1B03036303).

Keywords: Nickel • Palladium • Bimetallic • Alloy • Catalyst • Suzuki Coupling Reaction

[1] J. M. Thomas, *Angew. Chem. Int. Ed.* **1999**, *38*, 3588-3628.
[2] P. Das, D. Sharma, A. K. Shil, A. Kumari, *Tetrahedron Lett.* **2011**, *52*, 1176-1178.
[3] J. K. Nørskov, T. Bligaard, J. Rossmeisl, C. H. Christensen, *Nature Chem.* **2009**, *1*, 37-46.
[4] P. Munnik, P. E. de Jongh, K. P. de Jong, *Chem. Rev.* **2015**, *115*, 6687-6718.
[5] Z. Li, M. Li, Z. Bian, Y. Kathiraser, S. Kawi, *Appl. Catal. B Environ.* **2016**, *188*, 324-341.
[6] S. Tao, Y. Chen, H. Wang, J. Qiu, X. Wang, *J. Mater. Chem. A* **2016**, *4*, 6304-6312.
[7] P. Tang, Y. Chai, J. Feng, Y. Feng, Y. Li, D. Li, *Appl. Catal. A: Gen.* **2014**, *469*, 312-319.
[8] Z. Li, J. Chen, W. Su, M. Hong, *J. Mol. Catal. A: Chem.* **2010**, *328*, 93-98.
[9] B. Sheng, L. Hu, T. Yu, X. Cao, H. Gu, *RSC Adv.* **2012**, 2, 5520-5523.
[10] C. Tang, A.-E. Surkus, F. Chen, M.-M. Pohl, G. Agostini, M. Schneider, H. Junge, M. Beller, *Angew. Chem. Int. Ed.* **2017**, *56*, 16616-16620.
[11] C. C. C. Johansson Seechurn, M. O. Kitching, T. J. Colacot, V. Snieckus, *Angew. Chem. Int. Ed.* **2012**, *51*, 5062-5085.
[12] A. Balanta, C. Godard, C. Claver, *Chem. Soc. Rev.* **2011**, *40*, 4973-4985.
[13] M. Lamblin, L. Nassar-Hardy, J.-C. Hierso, E. Fouquet, F.-X. Felpin, *Adv. Synth. Catal.* **2010**, *352*, 33-79.
[14] J.-S. Chen, A. N. Vasiliev, A. P. Panarello, J. G . Khinast, *Appl. Catal. A: Gen.* **2007**, *325*, 76-86.
[15] T. Hattori, A. Tsubone, Y. Sawama, Y. Monguchi, H. Sajiki, *Catalysts* **2015**, *5*, 18-25.
[16] M. Kim, E. Heo, A. Kim, J. C. Park, H. Song, K. H. Park, *Catal. Lett.* **2012**, *142*, 588-593.
[17] C. M. Crudden, M. Sateesh, R. Lewis, *J. Am. Chem. Soc.* **2005**, *127*, 10045-10050.
[18] H.-Q. Song, Q. Zhu, X.-J. Zheng, X.-G. Chen, *J. Mater. Chem. A* **2015**, *3*, 10368-10377.

[19] C. Mateos, J. A. Rincón, B. Martín-Hidalgo, J. Villanueva, *Tetrahedron Lett.* **2014**, *55*, 3701.
[20] Z. Wang, W. Chen, Z. Han, J. Zhu, N. Lu, Y. Yang, D. Ma, Y. Chen, S. Huang, *Nano Res.* **2014**, *7*, 1254-1262.
[21] Y. Liu, X. Bai, S. Li, *Micropor. Mesopor. Mater.* **2018**, *260*, 40-44.
[22] Y. Wu, D. Wang, P. Zhao, Z. Niu, Q. Peng, Y. Li, *Inorg. Chem.* **2011**, *50*, 2046-2048.
[23] S. De, J. Zhang, R. Luque, N. Yan, *Energy Environ. Sci.* **2016**, *9*, 3314-3347.
[24] X.-L. Zhang, S.-H. Bao, Y.-C. Xin, X. Cao, P. Jin, *Front. Mater. Sci.* **2015**, *9*, 227-233.
[25] F.-S. Han, *Chem. Soc. Rev.* **2013**, *42*, 5270-5298.
[26] X. Li, X. Wang, M. Liu, H. Liu, Q. Chen, Y. Yin, M. Jin, *Nano Res.* **2018**, *11*, 780-790.
[27] L.-X. Ding, A.-L. Wang, Y.-N. Qu, Q. Li, R. Guo, W.-X. Zhao, Y.-X. Tong, G.-R. Li, *Sci. Rep.* **2013**, *3*, 1181.
[28] S. Jang, T. Kim, K. H. Park, *Catalysts* **2017**, *7*, 247.
[29] M. T. Reetz, R. Breinbauer, K. Wanninger, *Tetrahedron Lett.* **1996**, *37*, 4499-4502.
[30] A. Ohtaka, J. M. Sansano, C. Nájera, I. Miguel-García, Á. Berenguer-Murcia, D. Cazorla-Amorós, *ChemCatChem* **2015**, *7*, 1841-1847.
[31] D. Han, Z. Zhang, Z. Bao, H. Xing, Q. Ren, *Front. Chem. Sci. Eng.* **2018**, *12*, 24-31.
[32] R. Nie, J. Shi, W. Du, Z. Hou, *Appl. Catal. A: Gen.* **2014**, *473*, 1-6.
[33] L. Feng, H. Chong, P. Li, J. Xiang, F. Fu, S. Yang, H. Yu, H. Sheng, M. Zhu, *J. Phys. Chem. C* **2015**, *119*, 11511-11515.
[34] J. Saha, K. Bhowmik, I. Das, G. De, *Dalton Trans.* **2014**, *43*, 13325-13332.
[35] R. K. Rai, K. Gupta, S. Behrens, J. Li, Q. Xu, S. K. Singh, *ChemCatChem* **2015**, *7*, 1806-1812.
[36] S. U. Son, Y. Jang, J. Park, H. B. Na, H. M. Park, H. J. Yun, J. Lee, T. Hyeon, *J. Am. Chem. Soc.* **2004**, *126*, 5026-5027.
[37] Ö. Metin, S. F. Ho, C. Alp, H. Can, M. N. Mankin, M. S. Gültekin, M. Chi, S. Sun, *Nano Res.* **2013**, *6*, 10-18.
[38] H. R. Choi, H. Woo, S. Jang, J. Y. Cheon, C. Kim, J. Park, K. H. Park, S. H. Joo, *ChemCatChem* **2012**, *4*, 1587-1594.
[39] L. Kürti, B. Czakó, *Strategic Applications of Named Reactions in Organic Synthesis*, Elsevier, Dorecht, **2005**
[40] L. Gao, C. Wang, R. Li, Q. Chen, *Nanoscale* **2016**, *8*, 8355-8362.

10.1002/cctc.201801872

WILEY-VCH

Entry for the Table of Contents

COMMUNICATION

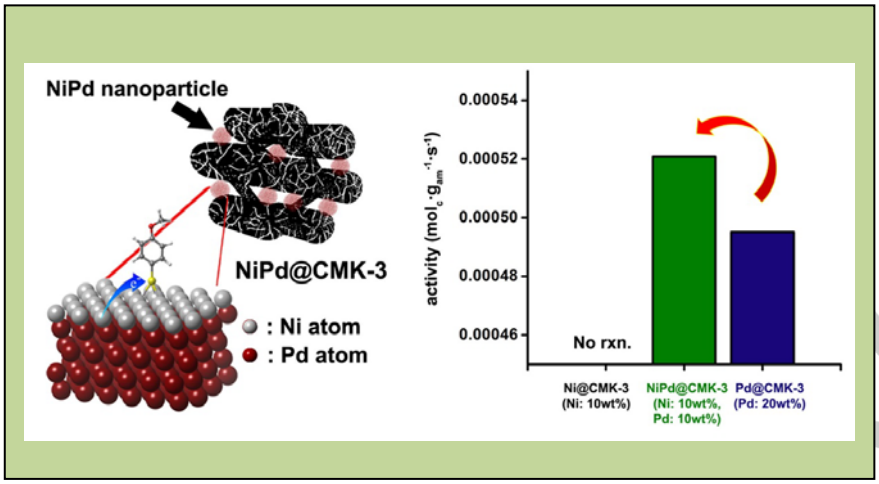

Ji Chan Park, Aram Kim, Sanha Jang, Jung-Il Yang, Shin Wook Kang, Chan-Woo Lee, Byung-Hyun Kim, Kang Hyun Park**

Page No. – Page No.

Facile synthesis of high performance NiPd@CMK-3 nanocatalyst for mild Suzuki-Miyaura coupling reactions